Enabling Reliable and Real-Time Packet Reception in User-Defined Overlapping LoRa Channels

Anonymous Authors

***Abstract*—In LoRaWAN, users are allowed to customize the center frequency of channel. This mechanism provides more flexibility but also introduces non-negligible interference for packet reception. This paper focuses on Overlapping Channel Interference (OCI), which arises when multiple users simultaneously transmit on partially overlapping channels. Existing methods proposed for interference in a single channel concurrently demodulate collided packets by inferring the chirp's onset and offset times. However, the collided chirps in OCI exhibit different center frequencies, leading to unpredictable chirp's onset and offset times which makes OCI particularly challenging to resolve. To resolve it, we propose Hole, a novel method to reliably receive target packet by exploiting the difference in chirp's onset and offset times instead of inferring them. Hole adopts signal elimination to construct identifiable energy losses for different chirps. Since the onset and offset times of target chirp are stable, its energy loss is deterministic while that of the interfering chirp is random. By comparing energy loss, we identify target chirp under OCI. However, in practice, the channel noise reduces the stability of energy loss. Therefore, we first theoretically analyze the optimal position of signal elimination and then propose noise-aware elimination setting. Furthermore, we also propose target packet recognition method by leveraging difference in packet's center frequency offset. The experiments in real LoRa network present that Hole improves the Packet Reception Rate (PRR) by up to 7.5× compared with existing methods.**

***Index Terms*—LoRa, LoRaWAN, Wireless Interference**

I. Introduction

As the most widely adopted protocol, LoRaWAN has been supported by more than 170 major mobile network operators worldwide [1]. To date, over 125 million LoRaWAN devices have been deployed to support various internet of things applications [2]. This rapid growth has imposed considerable pressure on limited available bandwidths. In major countries and regions, the uplink bandwidth is typically restricted to $8MHz$–$26MHz$ [3], while the minimum bandwidth occupied by a single device is $125kHz$. Hence, a pronounced asymmetry exists between the massive number of connected devices and the scarce spectral resources. Even worse, LoRaWAN allows users to freely configure Center Frequency (CF) of logical channel defined by the (BW,SF) pair of Bandwidth (BW) and Spreading Factor (SF), which inevitably leads to increased packet collisions in overlapping logical channels [1], [4].

As illustrated in Fig. 1, three independent LoRa networks coexist in neighboring area. Due to the lack of coordination, three end nodes EN_1, EN_2, and EN_3 are configured to use same logical channel with different CF to concurrently transmit packets. Hence, the packet reception of EN_2 in gateway GW_2 will be interfered by concurrent packets from EN_1 and EN_3. The caused interference manifests in two major aspects. On

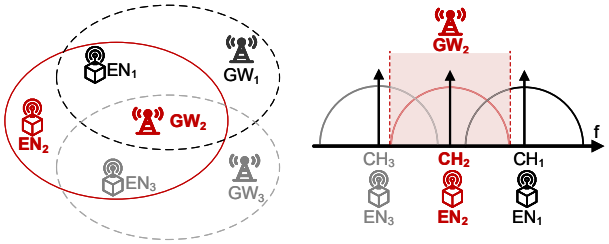

Fig. 1. Overlapping channel interference in coexisting LoRa networks.

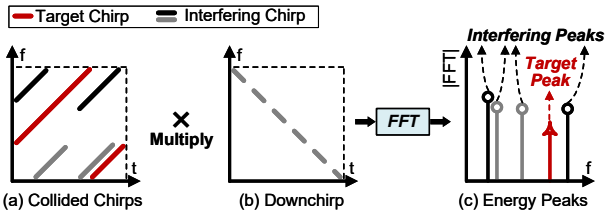

Fig. 2. OCI causes demodulation error in packet reception.

the one hand, if the interfering packets from EN_1 or EN_3 arrive at the gateway GW_2 earlier, the GW_2 will mistakenly lock onto the interfering packet, leading to the loss of the target packet. On the other hand, even if the packet from EN_2 is correctly locked, the interfering packets with higher power from EN_1 or EN_3 still cause demodulation errors. As shown in Fig. 2(a), collided chirps appear in the demodulation window. Standard LoRa demodulation multiplies the received chirp with downchirp to perform despreading in Fig. 2(b), which converts chirps into the single tone signal. In Fig. 2(c), Fast Fourier Transform (FFT) is applied to extract the intensity in each frequency. Then, the standard LoRa demodulation selects the highest energy peak and regards its corresponding frequency as the demodulation result. Hence, when any interfering chirp has higher power than the target chirp, the standard LoRa demodulation will incorrectly select the interfering energy peak, leading to demodulation errors. Therefore, *we define the interference among multiple overlapping logical channels as Overlapping Channel Interference (OCI).*

Existing studies primarily focus on resolving packet collisions that occur within a single logical channel, commonly referred as single channel interference. These works aim to enable concurrent demodulation by decomposing all collided packets. To this end, the above methods assume that the onset and offset times of all collided chirps remain stable and exploit various features to infer these boundaries. However, in the presence of OCI, where the center frequencies of interfering packets are random and unknown, interfering chirps only partially fall within the demodulation window of the target

chirp. Thus, the onset and offset times of such interfering chirps become inherently unpredictable because they depend on multiple random factors including the CF, packet arrival time, and the modulated symbol. Hence, the demodulation features used by existing methods such as energy peak ratio [5]–[9] and common energy peaks [10], [11] are unable to obtain the onset and offset times of interfering chirps, which causes failure in resolving OCI. Furthermore, most existing methods require the support of cloud radio access network with high cost and latency because the local gateway cannot store large number of I/Q samples and provide high computational capability to process signals. Hence, they cannot achieve real-time demodulation in gateway.

To achieve reliable packet reception under OCI, the new feature is required to enable real-time demodulation without accurate onset and offset times of collided chirps. We observe that even though precisely determining the onset and offset times of chirps is challenging, the difference in these times remains significant and stable. The target chirp fully occupies the demodulation window, whereas interfering chirps with different CF and arrival times only partially overlap with this window. To exploit this temporal discrepancy, we propose a novel operation termed time-domain signal elimination. Specifically, we observe that eliminating a fixed time segment from the received signal induces different proportions of energy loss for chirps with different onset and offset times. This energy loss is reflected by the reduction ratio of the energy peak before and after the signal elimination. For the target chirp whose onset and offset times are aligned with the window, the reduction ratio is deterministic and equals the ratio of the remaining chirp duration to the duration of window. In contrast, the incomplete interfering chirps, characterized by diverse onset and offset times, exhibit reduction ratios that differ markedly from that of the target chirp. Consequently, the target chirp can be reliably identified by comparing the reduction ratios of the corresponding energy peaks.

However, applying time-domain signal elimination still faces several challenges. First, under OCI, the interfering packets in same (BW, SF) as target packet may be incorrectly locked by gateway, resulting in the loss of the target packet. How to achieve real-time recognition of target packet is challenging. Second, within each window, blindly selecting the position (onset and offset times) of signal elimination causes the target and interfering chirps to experience similar energy losses, which generates similar reduction ratio and leads to demodulation error under the impact of channel noise. Therefore, how to determine the effectiveness of signal elimination in different positions is still challenging. Finally, in practice, the onset and offset times of interfering chirps are unknown, making it difficult to directly identify the optimal position for signal elimination. A brute-force search of all possible positions incurs prohibitive time overhead, violating real-time demodulation requirements. Hence, how to design a low-cost yet effective method to determine valid signal elimination is also challenging.

To cope with the above challenges, we propose Hole[1], a novel design to achieve reliable demodulation of target packets under OCI. First, we exploit difference in Center Frequency Offset (CFO) to prevent incorrect locking of interfering packet. For each received packet, we first despread its upchirp and downchirp. Then we utilize the resulting frequency shift and amplitude variation of energy peaks to rapidly determine the packet's CFO under the impact of interfering packets. Then, packet with CFO within the expected range are recognized as target. Second, we analyze the impact of invalid signal elimination on the demodulation under channel noise. We model the relationship between the position of signal elimination and the resulting energy loss of collided chirps. According to the model, we further determine the optimal position of signal elimination in theory. Finally, to balance time overhead and demodulation reliability, we employ multiple rounds of signal eliminations to approximate the performance of using the theoretically optimal position. The positions and rounds for signal elimination are adaptively selected based on noise intensity. Additionally, we incorporate the absolute energy intensity as auxiliary feature to refine demodulation results.

The contribution of this paper is summarized as follows.

- We propose Hole, a novel design to achieve real-time demodulation of LoRa packet under OCI. Hole adopts signal elimination which extracts difference in chirp's onset and offset times to identify target chirp.
- We resolve three practical challenges to reduce the occurrence of packet loss and enhance demodulation reliability. Hole can be easily deployed in existing LoRa networks because it doesn't require any modification in commercial LoRa nodes.
- The experimental results in real deployed LoRa network show that Hole can improve the PRR by up to 7.5× compared with existing methods under OCI.

The rest of this paper is organized as follows. We summarize the related work in Section II and introduce the motivation of our work in Section III. We then present the design of Hole in Section IV. We analyze the experimental results in Section V and finally conclude our work in Section VI.

II. Related Work

Numerous studies have focused on resolving single channel interference. Existing works can be broadly categorized into two classes: concurrency demodulation and collision avoidance. The key idea of concurrency demodulation is to decompose all collided packets. They rely on the assumption that the onset and offset times of all collided chirps remain predictable. Authors in [6]–[9] extract the onset and offset times of chirps by tracking the energy peak ratios across neighboring windows. Then they classify collided chirps into corresponding packets. Authors in [10], [11] divide the demodulation window based on the chirp onset times and infer chirp's duration by searching for common energy peaks. However, under OCI, interfering packets in user-defined channels have

[1]Time-domain signal elimination is like digging hole in window.

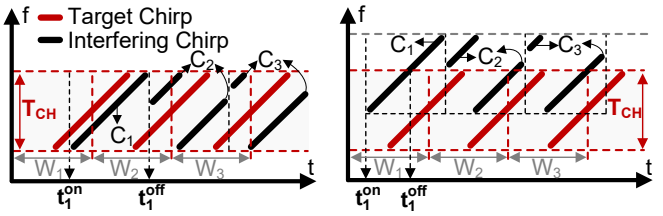

(a) Single channel interference. (b) Overlapping channel interference.

Fig. 3. Compared with single channel interference, interfering chirps in OCI have unpredictable onset and offset times.

random CF. Hence, the onset and offset times of interfering chirps depend not only on arrival time but also on their randomly modulated symbols. The energy peak ratios can only reflect the proportion of the chirp's duration within different windows. The onset and offset times of the chirps still remain unknown. Furthermore, most existing methods rely on the support of cloud radio access network. The local gateway typically lacks the storage capacity to buffer large volumes of I/Q samples and the computational resources required for signal processing [8]. As a result, real-time demodulation at the gateway is not feasible.

In contrast to concurrent demodulation, collision avoidance aims to ensure that at most one packet is transmitted within a single logical channel at any given time. To achieve this goal, existing methods primarily rely on centralized scheduling at the gateway or distributed channel occupancy detection at end nodes. Authors in [12], [13] adopt centralized allocation of logical channel usage at the LoRa gateway. However, such methods can only prevent collisions among nodes within a single LoRa network. In the presence of coexisting networks operated by independent users in adjacent areas, a single gateway cannot schedule transmissions or assign channels for devices belonging to other networks. Hence, centralized scheduling cannot effectively mitigate OCI. Studies in [14]–[16] propose using CSMA to sense occupancy of logical channel and then perform back-off. However, in densely deployed networks, CSMA significantly degrades transmission efficiency. Moreover, the adverse effects of hidden and exposed terminals on transmission reliability cannot be ignored.

III. Motivation

A. Limitation of Existing Methods

In OCI, the interfering chirps are incomplete in target chirp demodulation window. Hence, their onset and offset times are unpredictable. For single channel interference shown in Fig. 3(a), the onset and offset times of interfering chirps in one packet are stable. Hence, they can be inferred by demodulation feature such as energy peak ratio among neighboring demodulation windows. Specifically, the energy peak ratio of interference chirp C_1 in W_1 and W_2 is 1/3, which means that the duration of chirp C_1 in W_1 is 1/4 of the demodulation window. Its corresponding onset time t_1^{on} can be obtained by arrival time of packet. Then, the offset time t_1^{off} can be inferred by known t_1^{on} and duration.

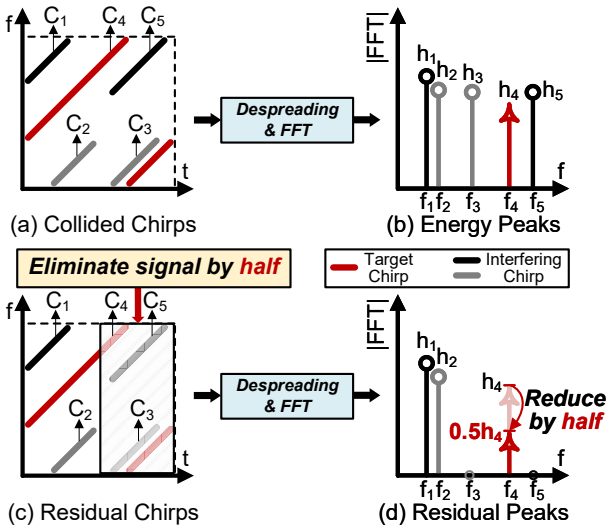

Fig. 4. Time-domain signal elimination construct identifiable energy loss for collided chirps. The reduction ratio of target peak is deterministic while that of interfering peak is random.

When OCI occurs, the duration and onset time of interfering chirps in two neighboring demodulation windows depend on the random CF, arrival time, and modulated symbol. For example, the interfering chirp C_1 only locates in W_1. The energy peak ratio in W_2 and W_1 is 0, which cannot reflect the duration of C_1 in each demodulation window. Meanwhile, to obtain the onset time of each chirp, existing methods require accurate arrival time of all collided packets. They need to reserve all I/Q samples that contain all collided packets and then perform packet-by-packet detection. However, in gateway with limited computational and storage capacity, it is difficult to detect interfering packets while demodulating the target packet in real-time LoRa demodulation process. Thus, the onset and offset times of interfering chirp cannot be obtained.

B. Our Insight

Within a demodulation window, the target chirp always occupies the entire window, whereas interfering chirps do not. This observation enables us to exploit the differences in onset and offset times to accurately identify the target chirp. To this end, we propose time-domain signal elimination, which identifies the target chirp by examining variations in the energy peaks after partially eliminating time-domain signals.

We take an example of collided chirps C_1 to C_5 in Fig. 4(a) to show the whole process. Fig. 4(b) presents the corresponding energy peaks after despreading and FFT. The energy peaks are located in different frequencies. The amplitude of each energy peak is denoted as h_1 to h_5. The energy peak in f_4 is target peak. To identify target peak, we eliminate the received signal by half the window to construct energy loss for different chirps. For C_4 which spans the whole demodulation window, the onset and offset times are known. Hence, its energy loss is predictable based on the duration of eliminated signals. Interfering chirps that only partially overlap with the demodulation window experience different energy losses.

To quantify the energy loss, we perform despreading and FFT to the residual chirps in Fig. 4(c) and present the results

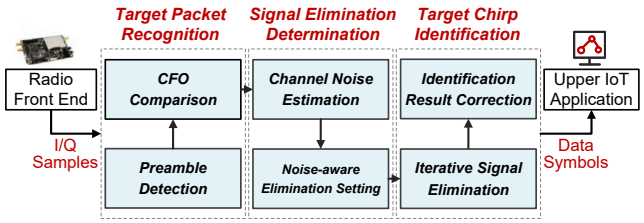

Fig. 5. Overview of Hole.

in Fig. 4(d). Only energy peak in f_4 reduces by half after signal elimination. The energy peaks in f_3 and f_5 disappear because the interfering chirps C_3 and C_5 are totally eliminated. Furthermore, the energy peaks in f_3 and f_5 are unchanged. By comparing the variations of energy peak, we regard the energy peak in f_4 as the target. In general demodulation, we apply time-domain signal elimination in each window and then regard the chirp whose energy peak's reduction ratio equals the ratio of the eliminated signal's duration to the whole window's duration as the target chirp.

IV. Design

We propose Hole, a novel design that uses time-domain signal elimination to achieve reliable and real-time demodulation for target packet under OCI. The whole procedure of Hole is illustrated in Fig. 5.

Target Packet Recognition. After receiving the original I/Q samples for radio front end, Hole relies on sliding window to detect preamble of received packets. To accurately recognize target packet, Hole uses upchirp and downchirp in each packet to perform despreading and FFT. Then, the frequency shift and amplitude variation of generated energy peak can reflect the CFO of packet. Hence, packet with CFO within the expected range are recognized as target.

Signal Elimination Determination. After locking the target packet, Hole will demodulate target chirp in current demodulation window. To balance the time overhead and demodulation reliability, Hole calculates the average SNR of the upchirps in preamble of target packet. Then Hole decides candidate positions and rounds of signal eliminations based on the intensity of channel noise.

Target Chirp Identification. Hole iteratively executes each signal elimination and tracks the variations of all energy peaks. Then the energy peak whose reduction ratio is the closest to the expected ratio will be regarded as the target peak. We also introduce absolute energy intensity to correct the result of identification. Finally, we take the frequency point where the target peak is located as the demodulation result. Hole will repeat the above process until all chirps are demodulated.

A. Target Packet Recognition

In the target channel, multiple interfering packets collide with target packet. The LoRa gateway will incorrectly lock interfering packet and cause loss of target packet. However, the packet detection proposed by existing studies [6], [10] cannot

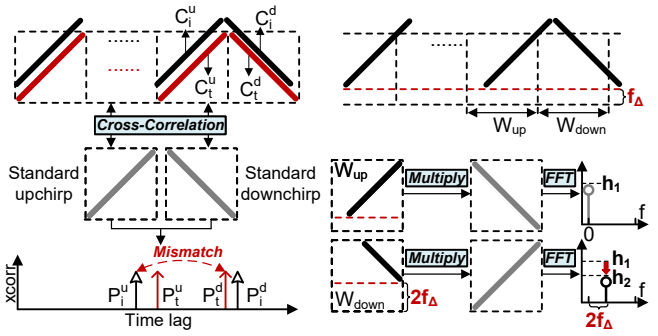

(a) Exsiting methods. (b) Our design.

Fig. 6. The difference in packet's CFO can be used to recognize target packet.

be directly reused. In Fig. 6(a), existing studies rely on cross-correlation between received signal and two chirps individually and then recognize packets by correlation peaks.

However, above strategy has two weaknesses. Firstly, it requires enough computational and storage capability to reserve numerous I/Q samples that including all packets and calculate cross-correlation, which makes it difficult to apply in real-time demodulation. Secondly, only relying on correlation peaks may cause erroneous decision of the beginning of chirps in payload. In Fig. 6(a), the chirps C_i^u, C_i^d, C_i^u and C_i^d generate four correlation peaks P_i^u, P_i^d, P_i^u and P_i^d. However, accurately matching the peaks of one packet is difficult. The mismatch of P_i^u and P_t^d leads C_i^u to be considering as the upchirp of target packet and then obtain error beginning of target chirps.

To cope with it, we leverage the different CFO to recognize target packet among collisions. In Fig. 6(b), after detecting the preamble by checking 8 continuous upchirp, Hole will individually despread chirps in W_{up} and W_{down}. By our measurements for commercial LoRa transceivers including SX1276 and SX1262, the CFO f_Δ of target packet is minor ($< 3kHz$) compared with bandwidth ($> 125kHz$). So we firstly check whether any energy peak appears in $[0, 6kHz]$ due to $2f_\Delta$ after despreading chirp in W_{down}. If no peak exists, the detected packet will be regarded as interfering packets. Otherwise, we check the amplitude of each appearing energy peak in $[0, 6kHz]$ because the energy peak of interfering packets may also appear in $2f_\Delta$. To avoid mismatch, we compare the ratio h_1/h_2 for all energy peaks in $[0, 6kHz]$. For target packet, its h_1/h_2 equals to $(bw - f_\Delta)/(bw - 2f_\Delta)$ where bw represents the bandwidth of target channel. Then, the energy peak whose ratio is in $[1, (bw - 3kHz)/(bw - 6kHz)]$ will be selected to calculate f_Δ and the beginning of chirps in target packet.

B. Signal Elimination Modeling

Within each demodulation window, we observe that time-domain signal elimination can be leveraged to extract difference in chirp's onset and offset times. However, blindly or randomly selecting the position for signal elimination leads to identification failure because it can induce similar energy losses across multiple chirps, thereby preventing reliable identification of the target chirp.

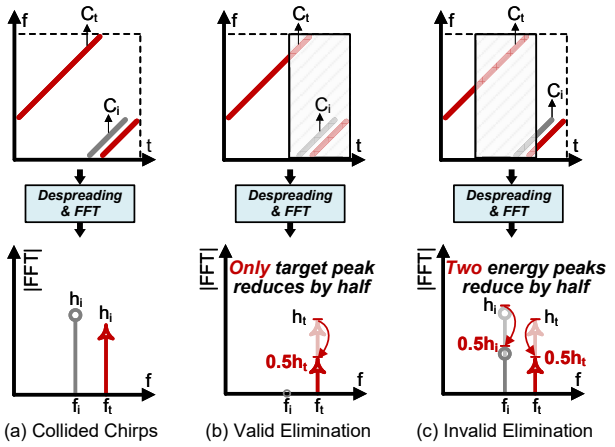

Fig. 7. Invalid signal elimination makes target chirp and interfering chirp experience same energy loss, which causes demodulation error.

We take an example of one target chirp C_t and one interfering chirp C_i in Fig. 7(a) to show the impact of invalid signal elimination. In Fig. 7(b) and (c), signal elimination is applied at different positions. After despreading and FFT, we observe that the amplitudes of both two energy peaks in Fig. 7(c) are reduced by half. As a result, the target peak cannot be identified among all energy peaks based on the energy peak's reduction ratio.

In above example, channel noise is ignored for simplicity. When channel noise is taken into account, the adverse effects of invalid signal elimination are significantly amplified, making reliable identification of the target chirp even more challenging. As illustrated in Fig. 8, when eliminating time-domain signal with duration $0.5T$, the expected reduction ratio R_t of target peak is 0.5. Hence, the received chirp whose reduction ratio is the closest to 0.5 will be regarded as target chirp. However, in the presence of channel noise, the actual reduction ratio $\overline{R}_t$ of target chirp deviates from its expected value and decreases to 0.45. Thus, the invalid signal elimination that causing failure of demodulation doesn't need to make the reduction ratio of interfering peak exactly equaling to 0.5. Instead, it suffices for the interfering peak's reduction ratio to fall within the interval $[0.45, 0.55]$.

To further present the impact of channel noise, we conduct experiments in real received LoRa signal. We configure 8 commercial LoRa nodes sending LoRa packets in $(125kHz, SF10)$ to generate overlapping channel interference. We implement one Software Defined Ratio (SDR) based LoRa gateway to receive collided packets. Then, we adopt random signal elimination to identify target LoRa chirp. We calculate the $E = |R_t - \overline{R}_t|$ of target packet and corresponding PRR under different Signal-to-noise Ratio (SNR). We control SNR by adjusting the transmitting power of LoRa nodes. Fig. 9(a) presents the cumulative distribution of E under different SNR, it is observed that lowering the SNR leads to an increase in the error E. The reason behind it is that higher channel noise makes the energy peak after FFT more unstable. The average E under (0,2)dB, (-5,-3)dB, and (-10,-8)dB is 0.06, 0.12, and 0.17, respectively. Fig. 9(b) shows the corresponding

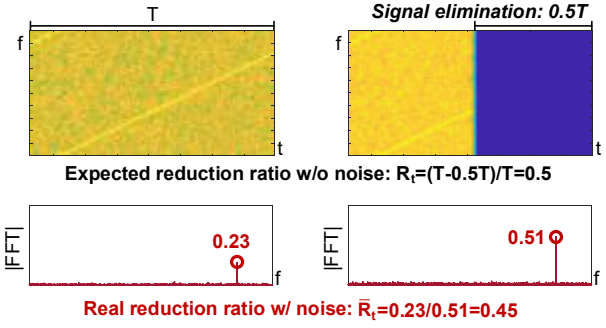

Fig. 8. Channel noise makes reduction ratio of energy peak unpredictable.

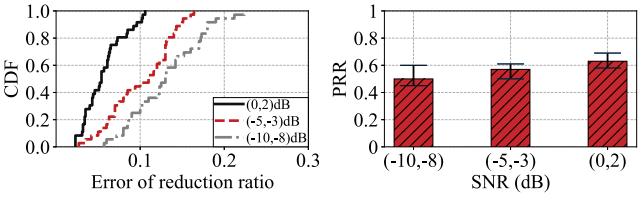

(a) E under different SNR. (b) PRR under different SNR.

Fig. 9. Adopting invalid signal elimination causes unreliable demodulation under channel noise.

PRR when using random signal elimination. When the SNR of target packet is in (0,2)dB, (-5,-3)dB, and (-10,-8)dB, the corresponding PRR is 0.49, 0.57, and 0.63, which cannot maintain the reliability of LoRa transmission.

In practice, we cannot predict and control the impact of noise to the energy peak. Hence, reducing E is difficult. In the whole process of signal elimination, the only issue we can control is R_t and R_i, where R_i represents the reduction ratio of interfering peak without noise. Hence, to enhance the reliability of demodulation, we require selecting the optimal position of signal elimination to maximize the distance $D = |R_i - R_t|$, which can make $\overline{R}_i$ as far away from R_t as possible, where $\overline{R}_i$ represents R_i under the impact of channel noise.

To maximize $D = |R_i - R_t|$, we first derive explicit expressions for R_i and R_t. We begin with a representative example in Fig. 7 to show the modeling process. Then we generalize the model to the practical scenario involving multiple collided chirps. R_i of interfering peak in D can be calculated by onset and offset times of C_i and the position of signal elimination. Fig. 10 summarizes all 5 distinct cases, t_e^{on} and t_e^{off} individually represent the onset and offset times of signal elimination. t_i^{on} and t_i^{off} denote the onset and offset times of interfering chirp C_i. Then we analyze these cases in turn.

Case 1 in Fig. 10(a) and Case 5 in Fig. 10(e) correspond to scenarios where signal elimination does not overlap with the interfering chirp. No energy loss is incurred and thus $R_i = 1$. For Case 2 in Fig. 10(b) and Case 4 in Fig. 10(d) where the signal elimination partially overlaps with the interfering chirp C_i, the corresponding R_i can be represented by

$$R_i = \begin{cases} 1 - \frac{t_e^{off} - t_i^{on}}{t_i^{off} - t_i^{on}}, \ t_e^{on} \in [0, t_i^{on}), t_e^{off} \in [t_i^{on}, t_i^{off}) \\ 1 - \frac{t_i^{off} - t_e^{on}}{t_i^{off} - t_i^{on}} \ t_e^{on} \in [t_i^{on}, t_i^{off}), t_e^{off} \in [t_i^{off}, T] \end{cases} \quad (1)$$

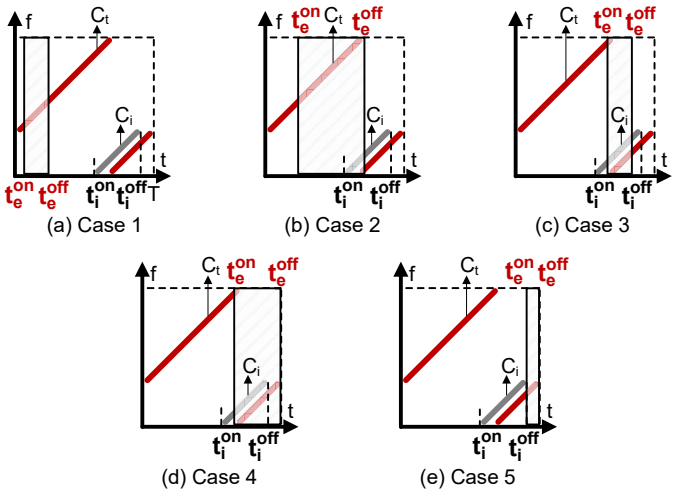

Fig. 10. 5 different cases of signal elimination.

For Case 3 in Fig. 10(c), the signal elimination is totally covered by the interfering chirp. The corresponding R_i is represented by

$$R_i = 1 - \frac{t_e^{off} - t_e^{on}}{t_i^{off} - t_i^{on}},\ t_e^{on} \in [t_i^{on}, t_e^{off}), t_e^{off} \in [t_i^{on}, t_i^{off}) \quad (2)$$

Compared with R_i, the value of R_t is easier to derive because the signal elimination is always fully covered by target chirp C_t. The corresponding R_t can be represented by

$$R_t = 1 - \frac{t_e^{off} - t_e^{on}}{T} \quad (3)$$

By above analysis, we derive R_i for each case and R_t. Since all expressions are linear, the maximum value of D can be obtained by taking the 1-order derivative. For brevity, we omit the detailed derivation and present the result directly. Specifically, When $t_e^{on} = t_i^{on}$ and $t_e^{off} = t_i^{off}$, D attains its maximum value $1 - (t_i^{off} - t_i^{on})/T$. In other words, the optimal position means that signal elimination completely overlaps with the interfering chirp. The above model only considers the scenario where two chirps collide. Facing more collided chirps, suppose that K interfering chirps appear in the demodulation window, we can independently obtain optimal position for each interfering chirp. Then we execute K times signal eliminations and regard the chirp whose reduction ratio is the closest to R_t across all signal eliminations as target chirp.

C. Signal Elimination Determination

In practice, directly obtaining the optimal position of signal elimination for each interfering chirp is challenging, as t_i^{on} and t_i^{off} is unknown. The most accurate way is to traverse all possible value of t_e^{on} and t_e^{off} and execute one signal elimination in each search. However, such naive traversal based search incurs prohibitive time overhead and fails to meet the real-time requirement of demodulation. To illustrate above challenge, consider the shortest chirp in $(125kHz, SF7)$ used by LoRaWAN, one target chirp demodulation window has 128 I/Q samples. The number of the (t_e^{on}, t_e^{off}) pairs is $\sum_{i=1}^{128} i = \frac{128(128+1)}{2} = 8,256$. It implies that LoRa gateway requires over 8 thousands of signal eliminations to demodulate one target chirp. Such a computational burden cannot be completed within the duration of one chirp on gateway with limited processing capability [8].

Based above analysis, an inherent balance exists between demodulation accuracy and time overhead in signal elimination. In Hole, the effectiveness of signal elimination is influenced by two factors: the intensity of channel noise and $D_{max} = 1 - (t_i^{off} - t_i^{on})/T$ which represents the maximum D when adopting signal elimination in optimal position. According to the equation of D_{max}, the interfering chirp with the maximum $t_i^{off} - t_i^{on}$ dominates the performance of adopting signal elimination. For clarity, we refer to this interfering chirp as the threat chirp. Consequently, the problem of finding optimal position of signal elimination can be simplified from considering all interfering chirps to focusing solely on the threat chirp. Nevertheless, this objective remains challenging because the t_i^{off} and t_i^{on} of the threat chirp are still unknown.

To address this challenge, we adopt a contrarian perspective on the original objective. We try to answer the following question: given different SNR, what is the minimum D_{max} required to achieve reliable demodulation using signal elimination? By minimum D_{max} (denoted by $\hat{D}_{max}$), the corresponding minimum duration $\hat{t}_i^{off} - \hat{t}_i^{on} = T \times (1 - \hat{D}_{max})$. If the actual $t_i^{off} - t_i^{on}$ of threat chirp is smaller than the minimum duration $\hat{t}_i^{off} - \hat{t}_i^{on}$, we can safely use $\hat{t}_i^{off} - \hat{t}_i^{on}$ to search optimal elimination because D_{max} of threat chirp always higher than the $\hat{D}_{max}$, ensuring reliable demodulation. The searching space of (t_e^{on}, t_e^{off}) will be lower than 2^{SF}. Otherwise, if $t_i^{off} - t_i^{on} \geq \hat{t}_i^{off} - \hat{t}_i^{on}$, it means that using signal elimination cannot accurately identify the target chirp under the impact of channel noise. An additional feature should be incorporated to assist in correcting the demodulation result.

We rely on real measurement to answer the above question about the $\hat{D}_{max}$. We configure two LoRa nodes to generate OCI and precisely control the transmission parameters to generate various SNR. Then we measure $\hat{D}_{max}$ for all (BW,SF) in LoRaWAN. When demodulating the target chirp, Hole firstly measures the SNR of target packet SNR_t by using 8 upchirps in preamble. Then, Hole obtains corresponding $\hat{D}_{max}$ and $\hat{t}_i^{off} - \hat{t}_i^{on}$ according to measurement result. After that, Hole searches the candidate positions of signal eliminations required to be executed and outputs them to the set $\mathbb{S} = \{s_1, s_2, s_3, ..., s_n\}, n \in [1, N]$. s_n contains the pair (t_e^{on}, t_e^{off}). t_e^{on} start from 0 and $t_e^{off} = t_e^{on} + (\hat{t}_i^{off} - \hat{t}_i^{on})$. The search will be ended when $t_e^{off} \geq T$.

D. Target Chirp Identification

Due to the limited computational capability of the gateway, we cannot execute all signal eliminations in set $\mathbb{S}$. To cope with it, Hole first evaluates the maximum number of signal eliminations M that the given computing hardware used by gateway can perform. Then Hole will selectively and literately execute signal elimination by the step $\delta = \lfloor M/N \rfloor$ such as s_1, $s_{1+\delta}$, and $s_{1+2\delta}$ until $n \geq N$. After all selected s_n is executed,

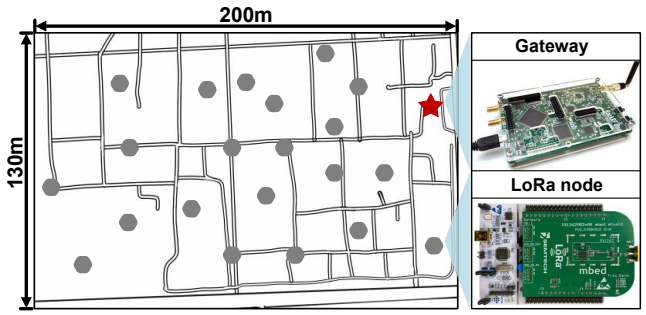

Fig. 11. Real deployed outdoor LoRa network.

the distance between R_t and reduction ratio of each energy peak will be recorded for comparison.

If any energy peak remains the closest to R_t in more than half of the executed signal eliminations, it is identified as target peak. Otherwise, we additionally introduce the absolute energy intensity as an auxiliary criterion to refine the demodulation result. We calculate the average amplitude of all energy peaks in the preamble and select the energy peak whose amplitude is closest to this average as the demodulation result. We literately execute above process until all target chirps are demodulated.

V. Evaluation

A. Experimental Setting

Implementation. We implement a prototype of Hole on an SDR-based LoRa gateway consisting of a USRP B210 as the RF front end and a laptop as the processing unit. The entire workflow of Hole is implemented using GNU Radio. After acquiring I/Q samples from the USRP B210, Hole performs real-time demodulation of the target packet and outputs the demodulated bytes to the upper layer. If not otherwise specified, the default central frequency of gateway is set to $490MHz$. The sampling frequency of gateway is set to $125kHz$, which matches the bandwidth of the target channel. All subsequent experiments are conducted in a real-world LoRa deployment. As illustrated in Fig. 11, the whole network contains 21 LoRa nodes, each node consists the LoRa module SX1262MB2CAS and microprocessor STM32L073RZ. The whole network is deployed in campus with area of $26{,}000m^2$. We configure one node as target node and the other 20 nodes as interfering nodes to generate OCI. The interfering node randomly decides its center frequency of transmission to partially overlap with target channel. The difference in center frequency of target node and interfering node is higher than 5% of target channel's bandwidth.

Baseline. To evaluate the effectiveness of Hole, we select 3 representative methods designed to address single channel interference as baselines for comparison. mLoRa [5] adopts successive interference cancellation to enable concurrent demodulation. It reconstructs complete chirps in the time domain based on detected energy peaks and iteratively eliminates decoded signals. CoLoRa [7] infers chirp onset and offset times by tracking the ratios of energy peaks across successive LoRa demodulation windows. CIC [10] divides the demodulation window according to detected chirp start times and performs FFT over sub-windows to estimate chirp onset and offset times. Notably, none of the above baselines support real-time demodulation on LoRa gateway. Therefore, we implement two parallel processing streams in GNURadio: one executes Hole in real time, while the other records the received I/Q samples for offline processing in MATLAB to run the baseline.

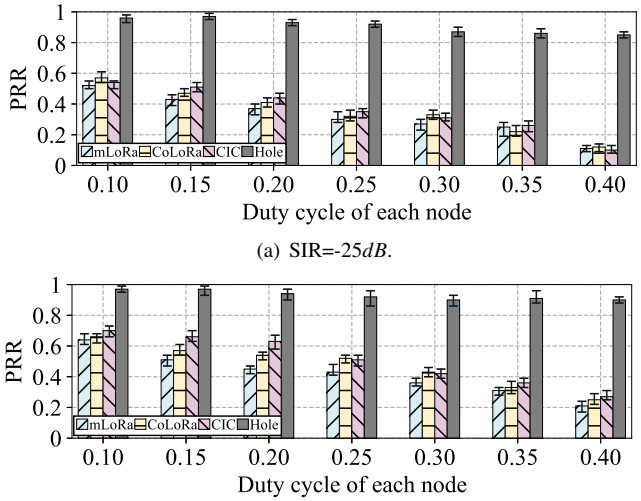

(a) SIR=-25dB.

(b) SIR=-15dB.

Fig. 12. Performance of 4 methods under different duty cycle and SIR.

B. Comparing with Existing Methods

In this section, we compare the performance of Hole with existing methods designed for resolving single-channel interference. As analyzed above, the unpredictable onset and offset times of collided chirps under OCI render existing methods ineffective for reliable demodulation. We conduct experiments in the real LoRa network to evaluate the PRR achieved by different methods. In each experimental round, one node is randomly selected as the target node, while the remaining nodes act as interfering nodes. All nodes are configured to transmit packets using $(125kHz, SF10)$, with the duty cycle varying from 0.10 to 0.40. In addition, we control the transmission power of all nodes to adjust the signal-to-interference ratio (SIR) of the target packet.

The experimental results are presented in Fig. 12(a) and (b) where the SIR is configured to -25dB and -15dB, respectively. As the duty cycle increases from 0.10 to 0.40, the PRR of all four methods decreases, since the higher duty cycles lead to more frequent packet collisions. In Fig. 12(a), when the duty cycle of each node increases to 0.40, the PRR of mLoRa, CoLoRa, and CIC drops to only 0.11, 0.12, 0.10, respectively. The key reason is that acquiring accurate onset and offset times of collided chirps is difficult. Such low PRR values are clearly insufficient to sustain reliable LoRa transmission in practical deployments. Oppositely, Hole can still achieve PRR of 0.85 at the duty cycle of 0.40. Across all duty cycle settings, the average PRR of Hole in all duty cycle is 0.90, which is 1.81×, 1.64×, and 1.51× higher than those of mLoRa, CoLoRa, and CIC. These results demonstrate that applying time-domain

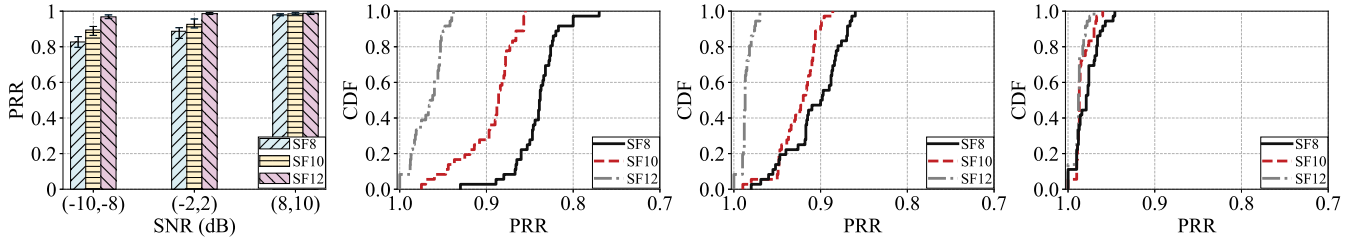

(a) PRR under different SNR. (b) (-10,-8)*dB*. (c) (-2,2)*dB*. (d) (8,10)*dB*.

Fig. 13. Packet demodulation performance of Hole under different SNR.

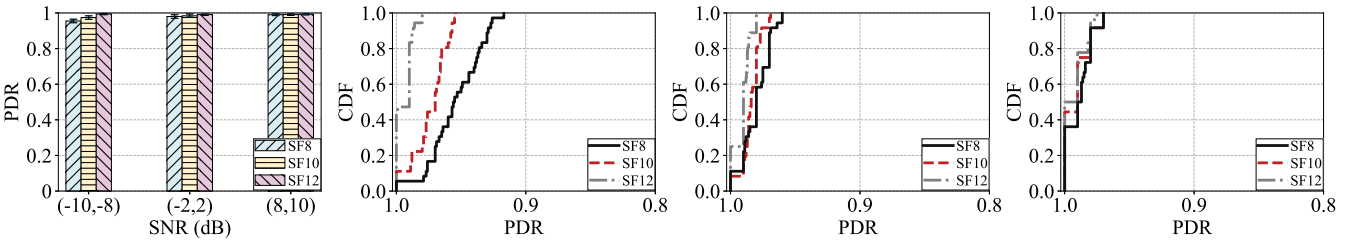

(a) PDR under different SNR. (b) (-10,-8)*dB*. (c) (-2,2)*dB*. (d) (8,10)*dB*.

Fig. 14. Packet detection performance of Hole under different SNR.

signal elimination can efficiently exploit the difference in chirp's onset and offset times, enabling robust identification of target chirp under severe collisions. In Fig. 12(b), even though the SIR increases to -15*dB*, the PRR of all three baselines is also significantly lower than Hole. The average PRR of mLoRa, CoLoRa, and CIC is 0.41, 0.47, and 0.51, which is 55.9%, 49.4% and 45.1% lower than Hole whose average PRR is 0.93. The above results confirm that Hole can significantly improve the reliability of the target LoRa link under OCI.

C. Basic Performance of Hole

We further evaluate the basic performance of Hole under different SNR. All LoRa nodes transmit packets with a fixed duty cycle of 0.20. The SNR of the target packet is controlled by adjusting the transmission power of the target node, while the bandwidth of all nodes is set to 125*kHz*. The experimental results are presented in Fig. 13 and Fig. 14. We individually calculate the PRR and PDR of target nodes under different SF and SNR levels. In Fig. 13(a), when using the same SF, the PRR achieved by Hole decreases as the SNR decreases. When SF is 8, the PRR under SNR=(8,10)*dB* is 0.96, which is 8.0% and 17.1% higher than the corresponding PRR under SNR=(-2,2)*dB* and SNR=(-10,-8)*dB* which is 0.89 and 0.82 respectively. This performance degradation is mainly caused by the noise with higher intensity, which destabilizes the energy peaks and causes failure in identifying target chirp.

Under same SNR, employing a higher SF significantly improves the PRR. This is because LoRa chirps with higher SF have longer duration, making them more resilient to channel noise. When the SNR is located in (-10,-8)*dB*, the PRR increases from 0.82 with SF8 to 0.89 with SF9 and further to 0.97 with SF10. Meanwhile, the PRR when using SF12 is stable when the SNR increases from (-10,-8)*dB* to (8,10)*dB*. In Fig. 13(b) and (c), we present the CDF (Cumulative Probability Distribution Function) of PRR under different SNR. When the SNR is (-10,-8)*dB* as shown in Fig. 13(b), the distribution of PRR in SF12 is the closest to 1. When the SNR is (8,10)*dB* as shown in Fig. 13(c), three curves are closer to each other. Overall, the experimental results show that Hole can maintain stable and reliable demodulation performance across a wide range of SNR and SF. For applications requiring high reliability, the user can select higher SF to cope with channel noise with high intensity.

In Hole, we introduce target packet recognition which leverages CFO among collided packets to accurately lock target packet. Hence, we also conduct experiments to verify the performance of packet recognition under different SNR. We measure Packet Detection Ratio (PDR) defined as the ratio between the number of locked target packets and the total number of target packets. The results are presented in Fig. 14(a)-(d). In Fig. 14(a),Hole consistently maintains a PDR above 0.95 across all SF and SNR, confirming that the proposed packet recognition is both stable and reliable in dynamic wireless environment. In Fig. 14(b)-(d), we also present the CDF of PDR in different SNR. Even though the SNR is located in (-10,-8)*dB*, Hole can still achieve PDR of 0.95, 0.97, and 0.99 when using SF8, SF10, and SF12, respectively. This high packet recognition accuracy provides a solid foundation for the subsequent demodulation process. As illustrated in Fig. 14(c) and (d), the PDR of all three SF further improves as the SNR increases, indicating strong robustness against channel noise.

D. Ablation Study

We also conduct ablation experiments to evaluate the effectiveness of key modules in Hole. We first verify the performance of noise-aware elimination setting which adaptively determines the position of signal elimination based on dynamic channel noise. For comparison, we implement Hole with random elimination setting, denoted as Hole w/o noise-aware

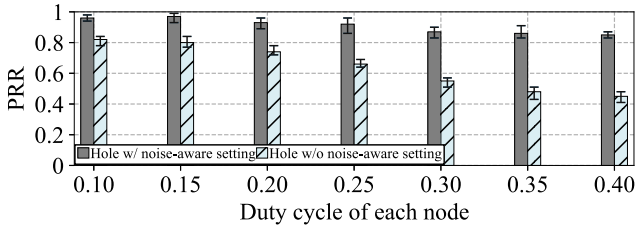

(a) Performance of noise-aware elimination setting.

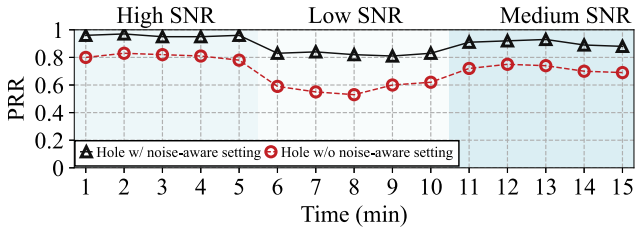

(b) Performance of Hole under dynamic environment.

Fig. 15. Adopting unsuitable signal elimination causes unreliable demodulation under channel noise.

setting. Fig. 15(a) presents the PRR under different duty cycle when individually executing two methods. All configurations are same as the experiment in Fig. 12(a). Across all duty cycle, the average PRR of Hole w/ noise-aware setting is 0.90, which 40.6% higher than the average PRR of Hole w/o noise-aware setting. When the duty cycle is 0.40, the PRR of Hole w/o noise-aware setting drops to 0.45, representing 47.0% reduction compared with the PRR of 0.85 achieved by Hole w/ noise-aware setting. These results indicate that using random elimination setting fails to extract the difference in onset and offset times of collided chirps. In contrast, it also shows that noise-aware signal elimination is efficient to select suitable elimination setting for demodulation.

We also evaluate the two methods in dynamic wireless environments. As illustrated in Fig. 15(b), the SNR of the target packets is varied across different time intervals. Low SNR, Mediudm SNR, and High SNR correspond to (-10,-8)dB, (-2,2)dB and (8,10)dB, respectively. Under high SNR, the average PRR of Hole w/ noise-aware setting is 0.96, which is 17.0% higher than the average PRR of Hole w/o noise-aware setting. When the SNR decreases, the average PRR of Hole w/o noise-aware setting sharply drops to 0.58 whereas Hole w/ noise-aware setting only decreases to 0.83. When SNR increases, the PRR of both two methods is improved but Hole w/ noise-aware setting is still higher. The results show that Hole can achieve reliable performance under dynamic wireless environment. Fig. 16 verifies the efficiency of identification result correction module. When this module is disabled (denoted as Hole w/o correction), the average PRR decreases to 0.84, which is 7.8% lower than the average PRR of Hole w/ correction.

VI. Conclusion

In this paper, we focus on resolving overlapping channel interference in LoRaWAN. Unlike existing methods that require

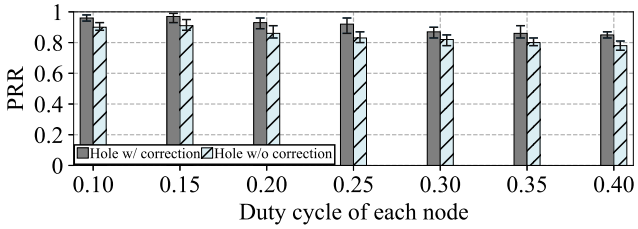

Fig. 16. Performance of identification result correction.

the accurate chirp's onset and offset time which is difficult to obtain, we propose Hole that adopts signal elimination which converts the difference in chirp's onset and offset times to identifiable energy loss to demodulate target chirp. To mitigate the impact of channel noise, we model the relationship between the position of signal elimination and the resulting energy loss. Then we theoretically derive the optimal position of signal elimination and propose noise-aware elimination setting used to balance the time overhead and demodulation reliability. We also achieve target packet recognition which leverages CFO to prevent locking interfering packets. The comprehensive experiments show that Hole can improve the PRR by up to 7.5× compared with existing methods.

References

[1] Semtech. (2025) Introduction of lorawan. [Online]. Available: https://www.adeunis.com/en/lorawan-private-vs-public-network-which-one-to-choose/

[2] Semtech. (2025) Lorawan® reaches critical mass: 125 million devices and accelerating growth. [Online]. Available: https://blog.semtech.com/lorawan-reaches-critical-mass-125-million

[3] L. A. T. Committee, "Lorawan™1.1 specification," LoRa Alliance, Technical Report, 2020.

[4] A. Gan, *LoRa-IoT NETWORK TECHNOLOGY*, 1st ed. Beijing: Tsinghua University Press, 2021.

[5] X. Wang, L. Kong, L. He, and G. Chen, "Mlora: A multi-packet reception protocol in lora networks," in *Proc. of IEEE ICNP*, 2019.

[6] S. Tong, J. Wang, and Y. Liu, "Combating packet collisions using non-stationary signal scaling in lpwans," in *Proc. of ACM MobiSys*, 2020.

[7] S. Tong, Z. Xu, and J. Wang, "Colora: Enabling multi-packet reception in lora," in *Proc. of IEEE INFOCOM*, 2020.

[8] Z. Xu, P. Xie, and J. Wang, "Pyramid: Real-time lora collision decoding with peak tracking," in *Proc. of IEEE INFOCOM*, 2021.

[9] X. Xia, Y. Zheng, and T. Gu, "Ftrack: Parallel decoding for lora transmissions," in *Proc. of ACM SenSys*, 2019.

[10] M. O. Shahid, M. Philipose, K. Chintalapudi, S. Banerjee, and B. Krishnaswamy, "Concurrent interference cancellation: decoding multi-packet collisions in lora," in *Proc. of ACM SIGCOMM*, 2020.

[11] Q. Chen and J. Wang, "Aligntrack: Push the limit of lora collision decoding," in *Proc. of IEEE ICNP*, 2021.

[12] L. Wang, X. Qi, R. Huang, K. Wu, and Q. Zhang, "Exploring partially overlapping channels for low power wide area networks," *ACM Transactions on Sensor Networks*, 2022.

[13] R. Hamdi, E. Baccour, A. Erbad, M. Qaraqe, and M. Hamdi, "Lora-rl: Deep reinforcement learning for resource management in hybrid energy lora wireless networks," *IEEE Internet of Things Journal*, vol. 9, no. 9, pp. 6458–6476, 2021.

[14] A. Gamage, J. C. Liando, C. Gu, R. Tan, and M. Li, "Lmac: Efficient carrier-sense multiple access for lora," in *Proc. of ACM MobiCom*, 2020.

[15] J. Ortín, M. Cesana, and A. Redondi, "How do aloha and listen before talk coexist in lorawan?" in *Proc. of IEEE PIMRC*, 2018.

[16] T.-H. To and A. Duda, "Simulation of lora in ns-3: Improving lora performance with csma," in *Proc. of IEEE ICC*, 2018.